0026-895X/04/6501-28–35$20.00
MOLECULAR PHARMACOLOGY
Copyright © 2004 The American Society for Pharmacology and Experimental Therapeutics
Mol Pharmacol 65:28–35, 2004

Vol. 65, No. 1
2668/1116467
Printed in U.S.A.

Measurement of Intermolecular Distances for the Natural Agonist Peptide Docked at the Cholecystokinin Receptor Expressed in Situ Using Fluorescence Resonance Energy Transfer

Kaleeckal G. Harikumar, Delia I. Pinon, William S. Wessels, Eric S. Dawson, Terry P. Lybrand, Franklyn G. Prendergast, and Laurence J. Miller

Mayo Clinic Scottsdale, Cancer Center and Department of Molecular Pharmacology and Experimental Therapeutics, Scottsdale, Arizona (K.G.H., D.I.P., L.J.M.); Mayo Clinic, Department of Molecular Pharmacology and Experimental Therapeutics, Rochester, Minnesota (W.S.W., F.G.P.), and Vanderbilt University, Department of Chemistry and Center for Structural Biology, Nashville, Tennessee (E.S.D., T.P.L.)

Received May 19, 2003; accepted September 26, 2003

This article is available online at http://molpharm.aspetjournals.org

ABSTRACT

Fluorescence resonance energy transfer is a powerful biophysical technique used to analyze the structure of membrane proteins. Here, we used this tool to determine the distances between a distinct position within a docked agonist and a series of distinct sites within the intramembranous confluence of helices and extracellular loops of the cholecystokinin (CCK) receptor. Pseudo–wild-type CCK receptor constructs having single reactive cysteine residues inserted into each of these sites were developed. The experimental strategy included the use of the full agonist, Alexa^{488}-CCK, bound to these receptors as donor, with Alexa^{568} covalently bound to the specific sites within the CCK receptor as acceptor. Site-labeling was achieved by derivatization of intact cells with a novel fluorescent methanethiosulfonate reagent. A high degree of spectral overlap was observed between receptor-bound donor and receptor-derivatized acceptors, with no transfer observed for a series of controls representing saturation of the receptor binding site with nonfluorescent ligand and use of a null-reactive CCK receptor construct. The measured distances between the fluorophore within the docked agonist and the sites within the first (residue 102) and third (residue 341) extracellular loops of the receptor were shorter than those directed to the second loop (residue 204) or to intramembranous helix two (residue 94). These distances were accommodated well within a refined molecular model of the CCK-occupied receptor that is fully consistent with all existing structure-activity and photoaffinity-labeling studies. This approach provides the initial insights into the conformation of extracellular loop regions of this receptor and establishes clear differences from analogous loops in the rhodopsin crystal structure.

An understanding of the molecular details of agonist ligand binding to a receptor provides powerful insights into the tertiary structure of the receptor in its active conformation, which, in turn, can afford valuable information for possible structure-based drug design. In this work, we have applied fluorescence resonance energy transfer (FRET) to the determination of distances between a fixed position in an agonist ligand and a series of defined positions within its receptor. Experimentally derived distance constraints so determined can complement insights gained from ligand structure-activity series (Ding et al., 2002) and studies using receptor mutagenesis (Kennedy et al., 1997; Gigoux et al., 1999) and photoaffinity labeling (Ji et al., 1997; Hadac et al., 1998, 1999; Ding et al., 2001). These experimentally determined intermolecular distances can also be extremely useful as constraints for three-dimensional model construction and refinement for receptor-ligand complexes.

The type A CCK receptor, a member of class I guanine nucleotide-binding protein (G protein)-coupled receptors, is normally activated by a linear peptide hormone. CCK is important for the regulation of nutritional homeostasis, playing roles in the stimulation of pancreatic exocrine secretion, gallbladder emptying, enteric motility, and satiety. Because of the physiological importance of this receptor and its validity as a drug target, there has been extensive work to elucidate its active conformation. The ligand structure-activity series (Bodanszky et al., 1977, 1980; Miller et al., 1981) have

This work was supported by grants from the National Institutes of Health (DK32878 to L.J.M.; NS33290 to T.P.L.) and the Fiterman Foundation.

ABBREVIATIONS: FRET, fluorescence resonance energy transfer; CCK, cholecystokinin; Alexa^{488}-CCK, Alexa^{488}-Gly-[(Nle^{28,31})CCK-26-33]; MTS, methanethiosulfonate; CHO, Chinese hamster ovary; KRH, Krebs-Ringers-HEPES; rms, root-mean-square.

clearly defined the pharmacophore of the natural ligand as the carboxyl terminal heptapeptide-amide and have demonstrated that a wide variety of modifications of the amino-terminal region of this peptide can be tolerated. Like many G protein-coupled receptors that bind small peptides, mutagenesis studies of the CCK receptor (Kennedy et al., 1997; Gigoux et al., 1999) have suggested the importance of the extracellular loop domains and the amino terminus (Ji et al., 1998). However, because mutagenesis experiments can provide only indirect structural information, these studies have not yielded unambiguous evidence for the mode of high-affinity binding of CCK to its receptor. The most direct insights to date have come from photoaffinity-labeling studies in the intact CCK receptor that have established specific ligand-receptor contact sites (Ji et al., 1997; Hadac et al., 1998, 1999; Ding et al., 2001).

Different groups have selected different subsets of these data to develop and support working models of the CCK-occupied receptor (Ding et al., 2002; Escrieut et al., 2002). Whereas all of these CCK receptor models share a general architecture of the receptor that is similar to the crystal structure of rhodopsin (Palczewski et al., 2000) and share the importance of the same regions of the CCK receptor amino terminus and extracellular loop regions (Ding et al., 2002; Escrieut et al., 2002), there are striking differences in the details of the docking of CCK. In one model that is formulated entirely from mutagenesis studies, the carboxyl terminus of CCK is situated within the confluence of transmembrane helices adjacent to transmembrane segment six (Escrieut et al., 2002). In our previously reported model for the high-affinity state of the CCK receptor that included photoaffinity-labeling constraints (Ding et al., 2002), the carboxyl terminus of CCK was positioned adjacent to the amino terminus of this receptor.

The results of the current work, which used FRET measurements to determine intermolecular distances between the ligand amino terminus and distinct residues within the receptor, were used to further refine our model, thus providing the most detailed picture for the high-affinity state of the CCK-receptor complex to date. These data and the corresponding refined structural model are consistent with all published results for the high-affinity agonist-receptor complex generated with a variety of experimental approaches. It is particularly important that the current structural constraints derived from the FRET experiments were determined with this receptor in its natural environment, after traversal of the cell's biosynthetic machinery, insertion into the plasma membrane, and ultimate display on the cell surface. Thus, all ancillary associated proteins involved in signal transduction or receptor regulation are also present in the experimental system, which facilitates functional assays. This natural environment is in sharp contrast with that in other approaches requiring the reconstitution of purified receptor protein in artificial lipid bilayers or of individual receptor ectodomain fragments in lipid micelles that are unlikely to represent the high-affinity, biologically active CCK-receptor complex.

Materials and Methods

Materials. Synthetic CCK (CCK-26-33), using the classic numbering convention based on CCK-33, was purchased from Peninsula Laboratories (Belmont, CA). 2-Aminoethyl-methanethiosulfonate hydrochloride was from Toronto Research Chemicals (Ontario, Canada). Alexa^{488}-*N*-hydroxysuccinimide and Alexa^{568}-*N*-hydroxysuccinimide were from Molecular Probes (Eugene, OR). All other reagents were analytical grade.

Preparation of Fluorescent Donor and Acceptors for FRET Studies. FRET studies require appropriate spectral properties in both donor and acceptor moieties, as well as favorable intermolecular spacing between donor and acceptor. For this project, we used an Alexa^{488} donor and an Alexa^{568} acceptor that have an appropriate spectral overlap, with 50% energy transfer at 62 Å (Fig. 1) (Panchuk-Voloshina et al., 1999).

The fluorescent donor was positioned at the amino terminus of a full agonist peptide ligand, Alexa^{488}-Gly-[(Nle^{28,31})CCK-26-33] (Alexa^{488}-CCK). There is strong precedent for the ability to successfully modify the amino terminus of CCK-26-33, the pharmacophoric domain of this hormone, without interfering with receptor binding or biological activity, using a broad variety of chemical groups that range from the natural peptide chain found in the longer forms of this hormone (Rosenzweig et al., 1983) to Bolton-Hunter reagent (Miller et al., 1981), a series of photolabile residues used in photoaffinity-labeling studies (Klueppelberg et al., 1990), and even to other fluorescent moieties such as rhodamine (Roettger et al., 1995, 2001), acrylodan (Harikumar et al., 2002), and 7-nitrobenz-2-oxa-1,3-diazol-4-yl (Harikumar et al., 2002). Alexa^{488}-CCK was recently shown to be a potent and fully effective agonist that binds specifically and saturably to the wild-type CCK receptor (Harikumar et al., 2002). In that work, the fluorescence properties of this probe were fully characterized, both while free in solution and when occupying its binding site within the CCK receptor (Harikumar et al., 2002). Here, we also have directly established the binding and biological activity (stimulation of intracellular calcium responses) characteristics of this ligand acting at the key CCK receptor mutants used in this study. These assays were performed as described previously (Harikumar et al., 2002; Ding et al., 2003).

The acceptor was an Alexa^{568} molecule covalently attached to specific engineered cysteine residues present within the ectodomain of the CCK receptor. The adducts containing Alexa^{568} were prepared by reaction of a thiol-selective fluorescent methanethiosulfonate

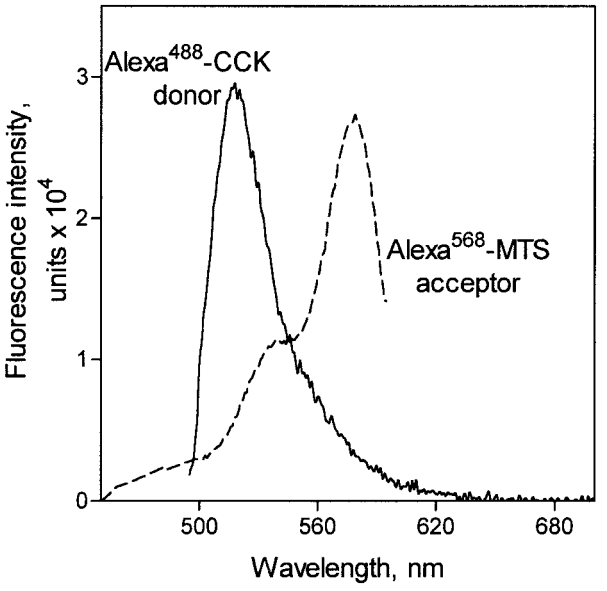

Fig. 1. Spectral overlap between the donor and acceptor. Shown are the spectra representing the emission of the donor, Alexa^{488}-CCK, when excited by light at 482 nm, and the absorption of the acceptor, Alexa^{568}. Adequate overlap exists between these two spectra to allow fluorescence energy transfer when the two molecules are in adequate spatial approximation.

(MTS) reagent (Alexa^{568}-MTS) with intact cells expressing a series of pseudo–wild-type CCK receptor constructs that were designed to each have a single reactive cysteine residue within a distinct receptor ectodomain (Ding et al., 2003) (Fig. 2). These monoreactive receptor constructs were prepared previously and characterized functionally (Ding et al., 2003). In one receptor construct, the reactive cysteine was present in transmembrane helix 2, near the extracellular surface (C94), whereas in the remaining three receptor constructs, a single reactive cysteine was incorporated into the first (N102C mutant), second (A204C mutant), and third (T341C mutant) extracellular loops.

The fluorescent reagent was specially prepared for the current study by acylation of the free amino group of 2-aminoethyl-methanethiosulfonate hydrochloride with Alexa^{568}-*N*-hydroxysuccinimide ester. The product of this reaction was purified to homogeneity using reverse-phase high-performance liquid chromatography. Here, we also characterized the mutant receptor constructs that had been derivatized with this reagent for their ability to bind and be activated by CCK, again using procedures that have been well-described previously (Harikumar et al., 2002; Ding et al., 2003).

Cell Culture. The receptor-expressing Chinese hamster ovary (CHO) cell lines were grown in tissue culture plasticware containing Ham's F-12 medium supplemented with 5% fetal clone-2 (Hyclone Laboratories, Logan, UT) in a humidified environment containing 5% carbon dioxide. Cells were passaged approximately twice per week.

Fluorescent Labeling of Cells Expressing Cysteine Mutant Receptors. CHO cell lines expressing the monoreactive cysteine mutants of the CCK receptor were detached using nonenzymatic cell dissociation medium (Sigma Chemical, St. Louis, MO). Intact cells were incubated with 1 μM Alexa^{568}-MTS reagent for 20 min at room temperature in Krebs-Ringer-HEPES (KRH) medium containing 25 mM HEPES, pH 7.4, 104 mM NaCl, 5 mM KCl, 2 mM $CaCl_2$, 1 mM KH_2PO_4, 1.2 mM $MgSO_4$, and 0.01% soybean trypsin inhibitor. Unreacted Alexa^{568}-MTS reagent was removed by centrifugation and washing. In a series of control experiments, the cells were incubated with 1 mM *N*-ethyl maleimide for 10 min before incubation with the Alexa^{568}-MTS reagent.

Alexa^{568}-labeled CCK receptor-bearing cells were incubated with 25 nM of Alexa^{488}-CCK for 2 h at 4°C in KRH medium containing 0.2% bovine serum albumin. Labeled cells were separated by centrifugation, washed with iced buffer, and resuspended in ice-cold KRH medium for FRET studies. One control condition represented this same labeling procedure in the presence of a 100-fold molar excess of nonfluorescent CCK.

Fluorescence Spectroscopy. Steady-state fluorescence was recorded using a SPEX Fluorolog spectrofluorophotometer (SPEX Industries, Edison, NJ) at 25°C using a 1-ml quartz cuvette. Fluorescence resonance energy transfer measurements were made using intact cells. Solvents and buffers were degassed by bubbling nitrogen to prevent quenching of fluorescence by soluble oxygen. Under the conditions used, fluorescence emission was also stable to photobleaching. After excitation at 482 nm, multiple emission spectra were accumulated between 490 and 700 nm (scanned at 0.3 s/nm). Unlabeled cells were used as a control to correct for background fluorescence and light scatter.

Fluorescence Resonance Energy Transfer. The distance (R) between the fluorophore within the Alexa^{488}-CCK peptide (donor) and the Alexa^{568}-CCK receptor (acceptor) was calculated using the Förster equation (Stryer and Haugland, 1967; Lakowicz, 1980). The

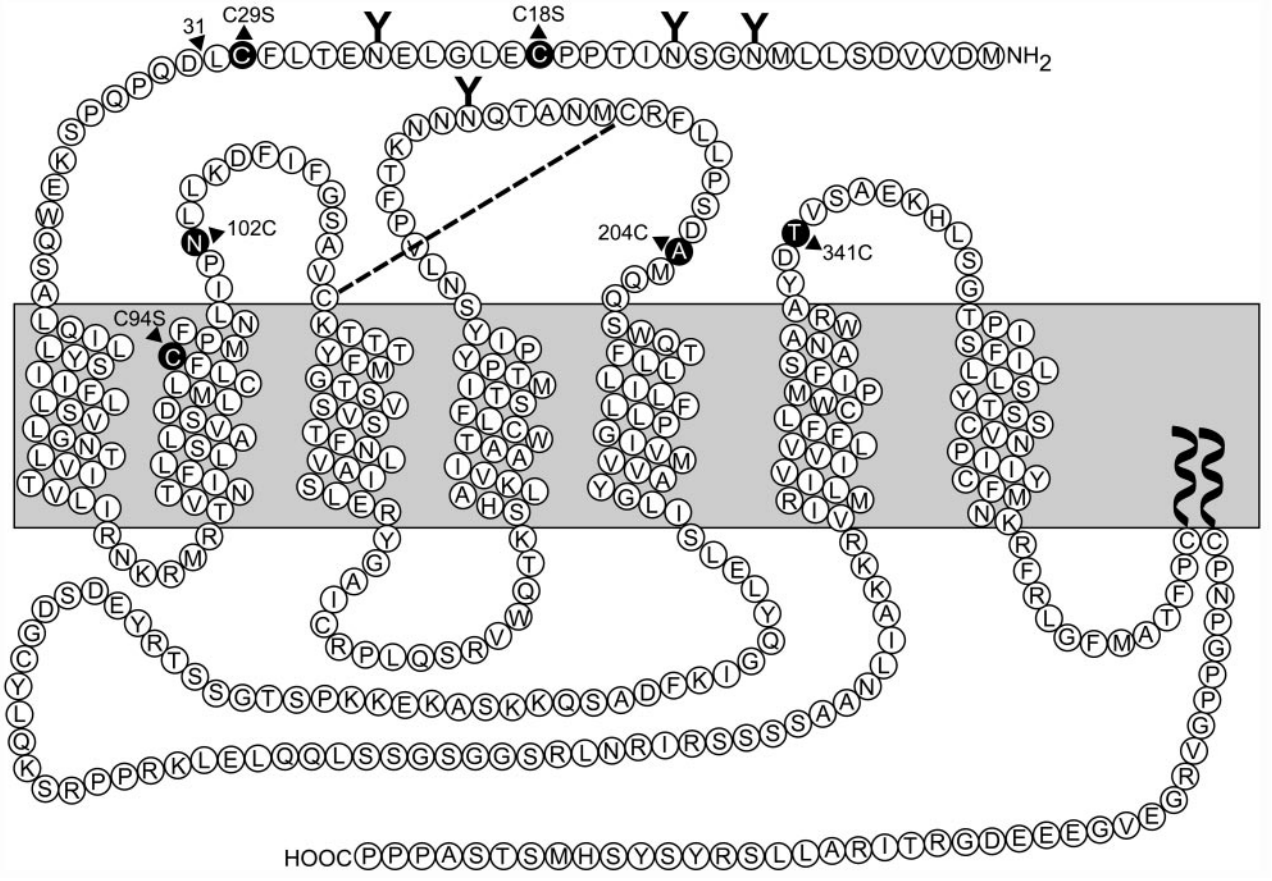

Fig. 2. CCK receptor constructs. Shown is a schematic diagram of the primary sequence of the rat type A CCK receptor, with the sites of introduction of reactive cysteine residues into the first, second, or third extracellular loop region or into the confluence of helices within transmembrane segment 2. The null cysteine-reactive CCK receptor mutant sequence included truncation of the amino terminus of the receptor at residue 31 and replacement of Cys^{94} with a Ser residue (Ding et al., 2003).

Förster critical distance (R_o) represents a constant that is characteristic of each donor-acceptor pair used for energy transfer and corresponds to the distance at which transfer efficiency is 50% between the donor and acceptor; $R_o = 9786(Jn^{-4}\kappa^2 Q_D)^{1/6}$ Å, where n is the refractive index of the medium (1.4 for the aqueous medium), and κ^2 is a geometric factor describing the relative orientation of the transition dipole of the donor and acceptor fluorophores. If donor and/or acceptor can exhibit isotropic dynamic orientation within the time scale of the fluorescence lifetime of the probes, then the orientation factor, κ^2, converges toward the value of ⅔. Support for the assignment of $\kappa^2 = ⅔$ was our previous report of evidence for rotational freedom of the receptor-bound probe and evidence for sufficient decay of anisotropy of this probe during the lifetime of donor emission (Harikumar et al., 2002). Those data demonstrated steady-state fluorescence anisotropy of 0.2 and time-resolved anisotropy with a decay value of 0.35 (r_o). Q_D is the fluorescence quantum yield of the donor in the absence of acceptor. For the Alexa^{488}-agonist, the quantum yield was measured from a comparison of emission intensities of sodium fluorescein in 0.1 N NaOH, using a quantum yield value 0.92 for fluorescein; J is the spectral overlap integral between donor emission [$F(\lambda)$] and acceptor absorbance [$\in(\lambda)$] spectra. It is calculated by the equation $J = \int F(\lambda)\in\lambda(\lambda)^4 d\lambda / \int F(\lambda) d\lambda$, where λ is the wavelength in centimeters, $F(\lambda)$ is the normalized and integrated fluorescence of the donor at wavelength λ, and $\in(\lambda)$ is acceptor absorption in absorbance units at wavelength λ for the overlapping area.

The efficiency of fluorescence energy transfer (E) was calculated from the fractional decrease in the fluorescence intensity of the donor (D) in approximation with the acceptor (A): $E = 1 - F_{DA}/F_D$, where F_{DA} and F_D are the fluorescence intensities of the donor (Alexa^{488}-CCK) in the presence and absence of the acceptor (Alexa^{568}-CCK receptor), respectively. Important controls used the same experimental conditions with the addition of a saturating concentration (100-fold molar excess) of nonfluorescent CCK competitor, as well as the use of the parental CHO cell line that did not express the CCK receptor but was labeled with the fluorescent reagent and incubated with the fluorescent donor ligand.

The efficiency of FRET is dependent on the inverse power of the distance between donor and acceptor (Lakowicz, 1980). With the calculated efficiency of transfer (E) the average proximal distance (R) between donor and acceptor was calculated by the equation $R = R_o[(1 - E)/E]^{1/6}$ Å, where R_o is the distance between donor and acceptor with an efficiency of energy transfer of 50%.

Molecular Modeling. Relevant residue-residue distances were determined for the CCK-receptor models proposed previously (Hadac et al., 1999; Ding et al., 2002) and compared with the analogous distances determined in the present studies using FRET.

In addition, the distances determined in the FRET experiments were used to further refine three-dimensional models of the CCK-receptor complex. For this refinement, the agonist peptide D-Tyr-Gly-(CCK-26-33) was initially fixed in its solution conformation (Fournie Zaluski et al., 1986) and docked manually into the receptor binding site. After limited energy minimization, the receptor-peptide complex was evaluated for consistency with the FRET distance measurements. Our previous molecular models indicated that the fluorophores at both donor and acceptor sites should possess considerable rotational freedom, and previous experimental measurements for steady-state fluorescence anisotropy and time-resolved anisotropy decay for the receptor-bound probe support this assumption (Harikumar et al., 2002). We generated initial estimates for the donor-acceptor distance constraints for molecular mechanics calculations based on Cβ (donor residue) to Cβ (acceptor residue) separation, because simple rotational sampling of fluorophores at the donor and acceptor sites in the molecular model suggests that these Cβ-to-Cβ measurements should yield a reasonable initial estimate for donor-acceptor distances, averaged over the accessible rotational states for the fluorophores. Relaxation of the minimized complex was performed with a series of 15-ps low-temperature (20 K) molecular dynamics simulations that used the collection of weak harmonic distance constraints described above to simultaneously refine the distances between the peptide ligand donor and each of the receptor acceptor sites (C94Cβ, N102Cβ, A204Cβ, and T341Cβ). The force constants governing these distance constraints were increased gradually from 1.0 to 15.0 kcal/mol/Å over the course of each simulation. The conformation of the peptide agonist was allowed to relax during these simulations; however, the conformation of the CCK receptor was maintained via a gradient of weak harmonic constraints applied to the peptide backbone atoms of the transmembrane-spanning residues (ranging from 1.0 to 10.0 kcal/mol/Å from exofacial to cytoplasmic ends, respectively). The exofacial loops were unconstrained during relaxation, except for the harmonic constraints taken from the FRET distance measurements described above.

Ensemble-averaged structures were calculated using a representative subset of conformers of the ligand-receptor complex that were extracted from molecular dynamics trajectory files and subjected to limited energy minimization to generate the final refined ligand-receptor complex model. Intermolecular distance approximations were then determined for each donor and acceptor fluorescent-probe pair in the peptide-receptor complex models. The centers of the fused-ring systems for each fluorescent probe were used as reference points to measure the final refined distances between individual donor-acceptor pairs. The impact of rotational and conformational freedom in the linker regions of each probe on these measurements was manually assessed using interactive graphics to estimate the upper and lower bounds for each of the refined distance measurements above.

The final model structure was evaluated for quality of side-chain packing, backbone geometry, and stereochemistry using the programs QPACK (Gregoret and Cohen, 1990) and PROCHECK (Laskowski et al., 1993). All manual model building, estimates of intermolecular distances, and root mean squared (rms) deviation calculations were performed with the interactive graphics program PSSHOW (E. Swanson, University of Washington, 1995). All energy minimization, molecular dynamics, and ensemble-averaged structure calculations were performed using the AMBER 7.0 suite of programs (Case et al., University of California San Francisco, San Francisco, CA). MD Display version 3.0 (Moth et al., Vanderbilt University, Nashville, TN) was used for visual analysis of molecular dynamics trajectories.

Statistical Analysis. Data were analyzed using Student's t test for unpaired values. Differences were considered significant at the $p < 0.05$ level.

Results

We have previously established and characterized the fluorescent ligand probe (Alexa^{488}-CCK) used in the present work and demonstrated that it is a potent and fully effective agonist that binds specifically and saturably to the wild-type CCK receptor (Harikumar et al., 2002). Here, we have extended this characterization and demonstrated similar binding characteristics at each of the receptor mutants used in this study, as well as its ability to stimulate a full biological response at those receptors ($p > 0.05$) (Table 1). In addition to performing the binding characterization at equilibrium, we evaluated the kinetics of association and dissociation to be certain that there were no differences from natural hormone ($p > 0.05$) (Table 2).

The monoreactive CCK receptor constructs used in this study were prepared previously and characterized functionally to demonstrate their ability to bind and signal in response to CCK like wild-type receptor (Ding et al., 2003). Here, we also extended this characterization to include their ability to bind ($p > 0.05$) and to elicit a full biological re-

TABLE 1

Binding and signaling characteristics of CCK ligands at CCK receptor constructs

Values represent means ± S.E.M. of data from a minimum of three independent experiments performed in duplicate. In the case of Alexa^{568}-receptor, the monoreactive CCK receptor-bearing cells were derivatized with 1 μ M Alexa^{568}-MTS for 20 min at room temperature and were used for radioligand binding assay or calcium-stimulation assay using CCK as the ligand.

	K_i		Stimulation of Intracellular Ca^{2+} EC_{50}	
	Alexa^{488} CCK	Alexa^{568}-Receptor (CCK)	Alexa^{488}-CCK	Alexa^{568}-Receptor (CCK)
	nM			
Wild-type	3.3 ± 1.3	N.D.	0.6 ± 0.1	N.D.
C94	7.0 ± 1.0	4.6 ± 1.5	0.6 ± 0.1	0.7 ± 0.2
N102C	1.7 ± 0.6	1.4 ± 0.4	0.9 ± 0.1	1.1 ± 0.4
A204C	12.5 ± 3.1	5.2 ± 3.8	0.4 ± 0.2	0.8 ± 0.2
T341C	10.3 ± 2.6	2.0 ± 0.3	0.7 ± 0.2	0.9 ± 0.2

N.D., not determined, because these lanes represent monoderivatized receptor constructs that were not possible for the wild-type CCK receptor. The wild-type CCK receptor binds CCK with a K_i = 1.0 ± 0.2 nM.

sponse after being derivatized with the Alexa^{568}-MTS reagent (Table 1).

Additional controls demonstrated that acceptor emission was dependent on excitation of the donor. Figure 3 shows typical fluorescence emission spectra obtained for cells expressing the N102C mutant CCK receptor labeled only with donor or acceptor fluorophores in the absence of the other (acceptor or donor). Cells expressing the wild-type CCK receptor occupied by Alexa^{488}-CCK were excited at 482 nm to yield a peak at 518 nm but demonstrated only minimal fluorescence at 603 nm. In addition, cells expressing monoreactive cysteine mutant receptors derivatized with the Alexa^{568}-MTS reagent demonstrated prominent fluorescence emission at 603 nm when excited at 578 nm, the region of the spectrum in which the donor would emit light if it were present. However, in the absence of donor, these cells exhibited negligible emission at 603 nm when excited at 482 nm. These spectra were typical of what was observed for each of the monoreactive CCK receptor mutants.

Key controls were also necessary in the dually labeled cells. The labeling procedure using Alexa^{568}-MTS would clearly be expected to derivatize cysteine residues on other membrane proteins not related to the CCK receptor. However, we reasoned that efficient FRET from the labeled agonist would occur only from the fluorescent adducts with the cysteine moieties intrinsic to the CCK receptor. The most critical control justifying this assumption was the cell-labeling and fluorescent ligand binding to CHO cells expressing the pseudo–wild-type CCK receptor devoid of a reactive thiol and to CHO cells expressing a monoreactive CCK receptor mutant, with comparison of the fluorescence spectra (Fig. 4). Derivatization of cysteine thiols occurred for both of these types of cells (bearing null-reactive and monoreactive CCK receptors), with fluorescence at 603 nm observed after excitation at 578 nm (data not shown). Similarly, both cells bound the fluorescence donor peptide as demonstrated by the peak in emission at 518 nm after excitation at 482 nm (Fig. 4). However, in the null cysteine-reactive CCK receptor-bearing cells, there was no FRET observed after excitation at 482 nm (Fig. 4). Absence of FRET was also reproduced in the monoreactive CCK receptor mutants that were treated with *N*-ethyl maleimide before attempting derivatization with the Alexa^{568}-MTS reagent (data not shown). Only in the monoreactive CCK receptor-bearing cells treated with this reagent under experimental conditions was significant energy transfer to the acceptor apparent, as exhibited by the peak fluorescence emission at 603 nm (data not shown).

FRET was determined for Alexa^{488}-CCK bound to cells expressing each Alexa^{568}-derivatized CCK receptor construct (those labeled at position 94 within the second transmembrane segment, at position 102 within the first extracellular

TABLE 2

Association and dissociation kinetics of CCK binding to CCK receptor constructs

Values represent means ± S.E.M. of data from three to four independent experiments performed in duplicate.

	K_{+1}	K_{-1}	K_d
	$min^{-1}\ nM^{-1}$	min^{-1}	*nM*
Wild-type	0.04 ± 0.01	0.04 ± 0.01	1.0 ± 0.2
C94	0.07 ± 0.01	0.04 ± 0.01	0.6 ± 0.1
N102C	0.04 ± 0.01	0.05 ± 0.01	1.6 ± 0.2
A204C	0.03 ± 0.01	0.05 ± 0.01	1.4 ± 0.5
T341C	0.03 ± 0.01	0.03 ± 0.01	1.0 ± 0.2

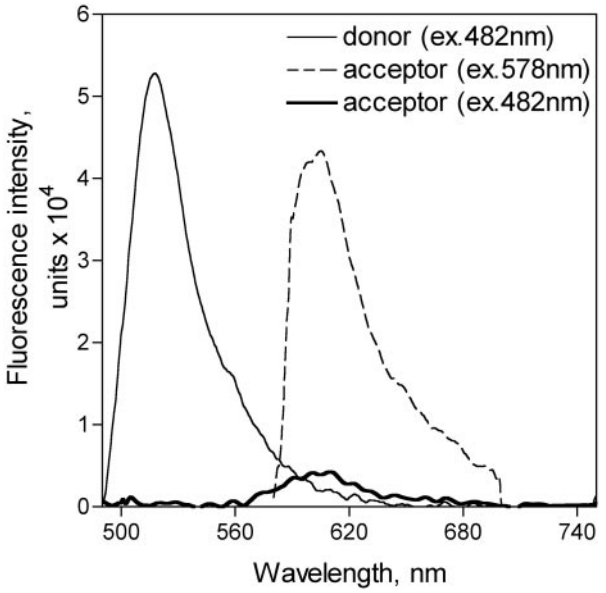

Fig. 3. Fluorescence emission spectra for cysteine-derivatized CCK receptor. Shown are three typical fluorescence emission spectra. Cells expressing the wild-type CCK receptor occupied by Alexa^{488}-CCK were excited at 482 nm to yield one spectrum. The second and third spectra represent cells expressing the N102C mutant CCK receptor derivatized with the Alexa^{568}-MTS reagent and excited at 578 or 482 nm. This demonstrates the negligible emission at 603 nm that can be expected from direct excitation of the acceptor by light at 482 nm in the absence of the Alexa^{488}-CCK donor.

loop, at position 204 within the second extracellular loop, and at position 341 within the third extracellular loop). Figure 4 shows a typical fluorescence emission spectrum for one of these constructs (N102C) in which clear fluorescence resonance energy transfer occurred. Each of the monoreactive CCK receptor mutants showed similar evidence of FRET. The fluorescence observed at 603 nm after excitation at 482 nm was negligible in the cells expressing the pseudo–wild-type CCK receptor devoid of a reactive thiol.

Fluorescence Resonance Energy Transfer Measurement. The extent of spectral overlap for each of the monoreactive CCK receptor constructs was calculated and is listed in Table 3. The highest degree of spectral overlap was observed between the fluorescent ligand and positions 102 and 341 within the CCK receptor. The Förster equation was used to quantify the distance between the fluorescent donor at the amino terminus of the CCK analog ligand and the fluorescent acceptor situated at these positions within the CCK receptor. Table 4 shows the efficiency of energy transfer between the Alexa^{488}-CCK and the Alexa^{568} receptor and the calculated distances for each of these constructs. The shortest distances were observed between the ligand and the first and third extracellular loops of the receptor.

Molecular Modeling. A previous peptide-CCK receptor complex model (Hadac et al., 1999; Ding et al., 2002) was used to predict the average distances (ligand residue 24 Cβ to engineered receptor Cys Cβ positions) expected for FRET measurements between donor and acceptor fluorophores, respectively. As can be seen from the data, three of four experimental donor-acceptor distances were predicted quite respectably by our previous model (Table 5). Only the ligand-receptor distance measured for the Alexa^{568}-derivatized A204C acceptor site was poorly predicted by this model.

Short, constrained molecular dynamics simulations were sufficient to refine our model so that it was fully consistent with all four intermolecular FRET distances measured in this study, as well as with previously published ligand structure-activity data, photoaffinity labeling, and mutagenesis results reported for the high-affinity CCK ligand-receptor complex (Dawson et al., 2002) (Fig. 5). Peptide ligand and receptor backbone conformational changes that occurred during structural refinement were monitored by calculating rms distance deviations. The receptor backbone in the transmembrane-spanning regions had an rms deviation from the starting structure (Fig. 5) of less than 1.0 Å, whereas the peptide backbone rms deviation was approximately 1.1 Å after relaxation. The backbone rms deviation for the exofacial loops and amino terminus was approximately 3.5 Å, primarily caused by the conformational change in the second exofacial loop required to satisfy the distance constraint for the acceptor at position 204 (Fig. 5). Structural validation results indicated that our refined model possesses the characteristics of a well-packed protein, with backbone dihedral angles and stereochemical parameters within acceptable ranges.

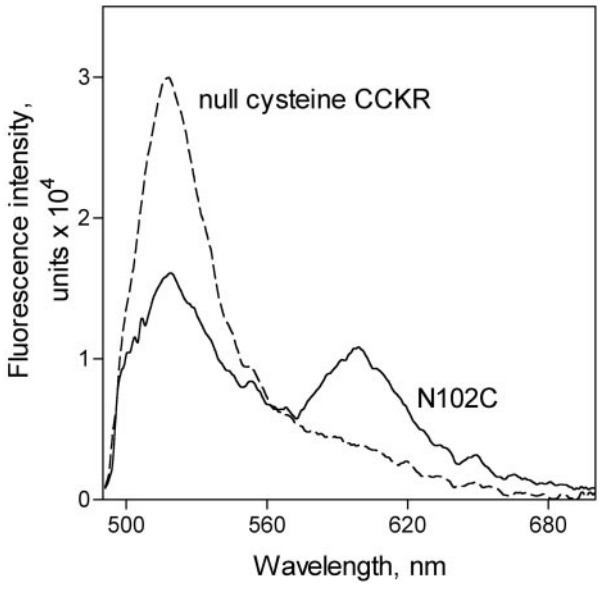

Fig. 4. Fluorescence emission spectra of null-reactive and N102C mutant CCK receptor constructs. CHO cell lines expressing the null-reactive or N102C mutant CCK receptor constructs were reacted with the Alexa^{568}-MTS reagent, as described under *Materials and Methods*. Receptors were then occupied with the Alexa^{488}-CCK, and this donor was excited at 482 nm. Shown is the peak of emission from this donor that was observed in the expected position of 518 nm. In the null-reactive CCK receptor-bearing cells, this energy was not transferred to the acceptor. Only in the monoreactive CCK receptor-bearing cells treated this way was significant energy transfer to the acceptor apparent. Shown is a typical emission spectrum from the N102C mutant, in which the acceptor emission was observed at 603 nm.

TABLE 3

Measured distance and the spectral overlap between donor Alexa^{488}-CCK and acceptor Alexa^{568}-receptor for cysteine mutants

Values are expressed as means ± S.E.M. of data from a minimum of five independent experiments.

CCK Receptor Mutant	R_o	$J \times 10^{-15}$
	Å	cm^3M^{-1}
C94	22 ± 1	4 ± 1
N102C	18 ± 0.2	4 ± 2
A204C	24 ± 2	10 ± 0.8
T341C	19 ± 1	2 ± 1

TABLE 4

Efficiency of energy transfer and the proximal distance between donor Alexa^{488}-CCK and acceptor Alexa^{568}-receptor for receptor constructs

Values are expressed as means ± S.E.M. of data from a minimum of five independent experiments.

CCK Receptor Mutant	Efficiency	R
	%	*Å*
C94	60 ± 3	21 ± 1
N102C	57 ± 3	17 ± 0.5
A204C	60 ± 4	22 ± 2
T341C	58 ± 4	18 ± 1

TABLE 5

Comparison of distances between donor and acceptor

Values for measured distances (R) are expressed as means ± S.E.M. (in Ångstroms) of data from a minimum of five independent FRET experiments. The predicted values are representative of the CCK receptor model complex before refinement using the FRET distance constraints, whereas the refined distance values and range (i.e., lower and upper distance bounds) reflect the final averaged structures for the complex obtained as described under *Materials and Methods*.

	Predicted	Measured	Refined	Range
		Å		
C94	26.5	21 ± 1	20.4	17–22
N102C	15.5	17 ± 0.5	14.6	13–19
A204C	32.6	22 ± 2	24.1	20–27
T341C	20.8	18 ± 1	18.5	13–25

Discussion

FRET is a powerful method for determining the distances between donor and acceptor (Stryer and Haugland, 1967). It has been used previously to analyze such distances between interacting soluble proteins (Garzon-Rodriguez et al., 1997; Rye, 2001) and between a soluble molecule and a purified, reconstituted membrane protein (Li et al., 1999; Vallotton et al., 2001). Site-directed spin-labeling has been used in a similar manner (Hubbell et al., 2003). In the present work, we have demonstrated the ability to apply FRET to a membrane receptor expressed in situ in the plasma membrane of an intact cell. This is particularly important because such a receptor system is fully functional, demonstrating normal agonist ligand binding, agonist-stimulated biological responses, and even agonist-stimulated regulatory processes (phosphorylation and internalization) (Roettger et al., 1995; Hadac et al., 1996; Rao et al., 1997).

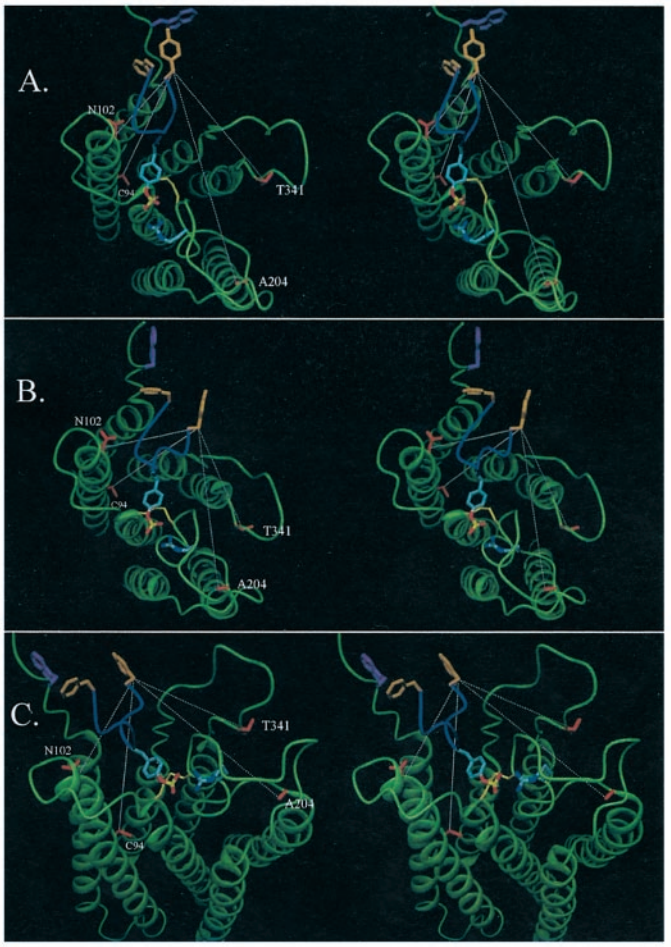

Fig. 5. Molecular model of the peptide-receptor complex before and after refinement of FRET-determined intermolecular distances. A, a stereo view for the peptide agonist-receptor complex derived from previous modeling work (Hadac et al., 1999). The peptide agonist backbone (blue) is highlighted along with three important peptide side chains, the N-terminal Tyr^{24} and C-terminal Phe^{33} (both in orange), as well as (SO_3)H-Tyr^{27} (multicolored). In the receptor, the established site of (pNO_2)-Phe^{33} covalent photolabel attachment, W39 (violet), the charge-charge pair R197:(SO_3)H-Tyr^{27} (multicolored), and the $Alexa^{568}$-labeled amino acid positions (red) are also highlighted. The predicted distances (Table 5) between pairs of donor and acceptor fluorophore-labeled amino acid positions are shown (white hashed lines). B, a stereo view of the peptide-receptor complex from the extracellular surface after refinement with distance constraints derived from the FRET experiments. The coloring scheme is as described for A. C, a stereo view of the refined peptide-receptor complex from an oblique angle relative to the lipid bilayer surface for improved perspective. All stereo views were created with the graphics package DINO (http://www.dino3d.org).

The approach we used was quite simple and should be amenable to many other plasma membrane receptors. Key was the production of a pseudo–wild-type receptor construct that was devoid of reactive extracellular thiol moieties (Ding et al., 2003). This was a useful template to engineer reactive cysteine residues in important extracellular domains (Ding et al., 2003). Multiple sequence alignments with CCK receptors from other species and closely related G protein-coupled receptors provided useful guidance to choose sites for cysteine insertion that were unlikely to interfere with receptor function. Indeed, these constructs bound CCK normally and signaled in response to agonist normally (Ding et al., 2003).

Particularly interesting was that the four intermolecular distances determined in these FRET studies were compatible with the independently derived molecular model we published previously (Ding et al., 2002). That earlier model was derived from existing structure-activity data for both peptide ligand and receptor, as well as from multiple photoaffinity-labeling constraints (Ji et al., 1997; Hadac et al., 1998, 1999; Ding et al., 2001). The FRET data were subsequently used to further refine our best previous working model of the agonist-occupied CCK receptor (Ding et al., 2002). The major structural difference that emerged from the refinement process entailed the conformation of the second extracellular loop. This loop is partially constrained by a disulfide bond with a cysteine in the first extracellular loop. The region within the second loop between this disulfide bond and the beginning of transmembrane segment five is 12 residues long, providing substantial opportunity for flexibility. Very little is known about the conformation of the loop regions of receptors in this superfamily, but it has recently been proposed that the extracellular loops in G protein-coupled receptors that bind peptide ligands probably adopt quite different conformations than those observed in the rhodopsin crystal structure (Ding et al., 2002). The current project provides experimental evidence for this hypothesis.

Future FRET experiments with donor and acceptor fluorophores placed in alternate positions in ligand and receptor will provide additional intermolecular distance measurements that can be used to further refine the receptor-agonist complex structure. Analogous experiments with peptide antagonists will allow us to begin to characterize some of the structural differences between active (i.e., agonist-bound) and inactive (i.e., antagonist-bound) receptor conformations. In principle, time-resolved fluorescence resonance energy transfer experiments can also be used to provide insights into dynamic changes in receptor conformation that are induced by agonist binding, and it may be possible to correlate these observed conformational changes with signaling and regulatory events controlled by receptor activation.

We believe the studies reported here indicate that FRET can be a powerful technique to provide quantitative structural information for G protein-coupled receptor/ligand complexes in cases in which X-ray crystallography or nuclear magnetic resonance spectroscopy are not practical at present. As such, FRET should become an important tool for future structural studies for G protein-coupled receptors and many other integral membrane receptors as well.

Acknowledgments

We thank Peter J. Callahan, Elizabeth M. Hadac, Eileen Holicky, and Susan Kuntz for technical assistance in these studies, and Elizabeth M. Hadac for help in preparation of figures.

References

Bodanszky M, Natarajan S, Hahne W, and Gardner JD (1977) Cholecystokinin (pancreozymin). 3. Synthesis and properties of an analogue of the C-terminal heptapeptide with serine sulfate replacing tyrosine sulfate. *J Med Chem* **20:**1047–1050.

Bodanszky M, Tolle JC, Gardner JD, Walker MD, and Mutt V (1980) Cholecystokinin (pancreozymin). Synthesis and properties of the N alpha-acetyl-derivative of cholecystokinin 27–33. *Int J Pept Protein Res* **16:**402–411.

Dawson ES, Henne RM, Miller LJ, and Lybrand TP (2002) Molecular models for cholecystokinin-A receptor. *Pharmacol Toxicol* **91:**290–296.

Ding XQ, Dolu V, Hadac EM, Holicky EL, Pinon DI, Lybrand TP, and Miller LJ (2001) Refinement of the structure of the ligand-occupied cholecystokinin receptor using a photolabile amino-terminal probe. *J Biol Chem* **276:**4236–4244.

Ding XQ, Dolu V, Hadac EM, Schuetz M, and Miller LJ (2003) Disulfide bond structure and accessibility of cysteines in the ectodomain of the cholecystokinin receptor: specific mono-reactive receptor constructs examine charge-sensitivity of loop regions. *Recept Channel* **9:**83–91.

Ding XQ, Pinon DI, Furse KE, Lybrand TP, and Miller LJ (2002) Refinement of the conformation of a critical region of charge-charge interaction between cholecystokinin and its receptor. *Mol Pharmacol* **61:**1041–1052.

Escrieut C, Gigoux V, Archer E, Verrier S, Maigret B, Behrendt R, Moroder L, Bignon E, Silvente-Poirot S, Pradayrol L et al. (2002) The biologically crucial C terminus of cholecystokinin and the non-peptide agonist SR-146, 131 share a common binding site in the human CCK1 receptor. Evidence for a crucial role of Met-121 in the activation process. *J Biol Chem* **277:**7546–7555.

Fournie Zaluski MC, Belleney J, Lux B, Durieux C, Gerard D, Gacel G, Maigret B, and Roques BP (1986) Conformational analysis of cholecystokinin (CCK-26-33) and related fragments by ^{1}H NMR spectroscopy, fluorescence- transfer measurements and calculations. *Biochemistry* **25:**3778–3787.

Garzon-Rodriguez W, Sepulveda-Becerra M, Milton S, and Glabe CG (1997) Soluble amyloid Aβ-(1–40) exists as a stable dimer at low concentrations. *J Biol Chem* **272:**21037–21044.

Gigoux V, Maigret B, Escrieut C, Silvente-Poirot S, Bouisson M, Fehrentz JA, Moroder L, Gully D, Martinez J, Vaysse N et al. (1999) Arginine 197 of the cholecystokinin-A receptor binding site interacts with the sulfate of the peptide agonist cholecystokinin. *Protein Sci* **8:**2347–2354.

Gregoret LM and Cohen FE (1990) Novel method for the rapid evaluation of packing in protein structures. *J Mol Biol* **211:**959–974.

Hadac EM, Ghanekar DV, Holicky EL, Pinon DI, Dougherty RW, and Miller LJ (1996) Relationship between native and recombinant cholecystokinin receptors: role of differential glycosylation. *Pancreas* **13:**130–139.

Hadac EM, Ji ZS, Pinon DI, Henne RM, Lybrand TP, and Miller LJ (1999) A peptide agonist acts by occupation of a monomeric G protein-coupled receptor: dual sites of covalent attachment to domains near TM1 and TM7 of the same molecule make biologically significant domain-swapped dimerization unlikely. *J Med Chem* **42:**2105–2111.

Hadac EM, Pinon DI, Ji Z, Holicky EL, Henne R, Lybrand T, and Miller LJ (1998) Direct identification of a second distinct site of contact between cholecystokinin and its receptor. *J Biol Chem* **273:**12988–12993.

Harikumar KG, Pinon DI, Wessels WS, Prendergast FG, and Miller LJ (2002) Environment and mobility of a series of fluorescent reporters at the amino terminus of structurally related peptide agonists and antagonists bound to the cholecystokinin receptor. *J Biol Chem* **277:**18552–18560.

Hubbell WL, Altenbach C, Hubbell CM, and Khorana HG (2003) Rhodopsin structure, dynamics, and activation: a perspective from crystallography, site-directed spin labeling, sulfhydryl reactivity and disulfide cross-linking. *Adv Protein Chem* **63:**243–290.

Ji TH, Grossmann M, and Ji I (1998) G protein-coupled receptors. I. Diversity of receptor-ligand interactions. *J Biol Chem* **273:**17299–17302.

Ji Z, Hadac EM, Henne RM, Patel SA, Lybrand TP, and Miller LJ (1997) Direct identification of a distinct site of interaction between the carboxyl-terminal residue of cholecystokinin and the type A cholecystokinin receptor using photoaffinity labeling. *J Biol Chem* **272:**24393–24401.

Kennedy K, Gigoux V, Escrieut C, Martinez J, Moroder L, Frehel D, Gully D, Vayse N, and Fourmy D (1997) Identification of two amino acids of the human cholecystokinin-A receptor that interact with the N-terminal moiety of cholecystokinin. *J Biol Chem* **272:**2920–2926.

Klueppelberg UG, Powers SP, and Miller LJ (1990) The efficiency of covalent labeling of the pancreatic cholecystokinin receptor using a battery of cross-linkable and photolabile probes. *Receptor* **1:**1–11.

Lakowicz JR (1980) Fluorescence spectroscopic investigations of the dynamic properties of proteins, membranes and nucleic acids. *J Biochem Biophys Method* **2:**91–119.

Laskowski RA, MacArthur MW, Moss DS, and Thornton JM (1993) PROCHECK. *J Appl Crystallogr* **26:**283–291.

Li M, Reddy LG, Bennett R, Silva ND Jr, Jones LR, and Thomas DD (1999) A fluorescence energy transfer method for analyzing protein oligomeric structure: application to phospholamban. *Biophys J* **76:**2587–2599.

Miller LJ, Rosenzweig SA, and Jamieson JD (1981) Preparation and characterization of a probe for the cholecystokinin octapeptide receptor, Nα(^{125}I-desaminotyrosyl-)CCK-8 and its interactions with pancreatic acini. *J Biol Chem* **256:**12417–12423.

Palczewski K, Kumasaka T, Hori T, Behnke CA, Motoshima H, Fox BA, Trong IL, Teller DC, Okada T, Stenkamp RE, et al. (2000) Crystal structure of rhodopsin: a G protein-coupled receptor. *Science (Wash DC)* **289:**739–745.

Panchuk-Voloshina N, Haugland RP, Bishop-Stewart J, Bhalgat MK, Millard PJ, Mao F, Leung WY, and Haugland RP (1999) Alexa dyes, a series of new fluorescent dyes that yield exceptionally bright, photostable conjugates. *J Histochem Cytochem* **47:**1179–1188.

Rao RV, Roettger BF, Hadac EM, and Miller LJ (1997) Roles of cholecystokinin receptor phosphorylation in agonist-stimulated desensitization of pancreatic acinar cells and receptor-bearing Chinese hamster ovary cholecystokinin receptor cells. *Mol Pharmacol* **51:**185–192.

Roettger BF, Hellen EH, Burghardt TP, and Miller LJ (2001) Multiple ligand and cell-dependent states of lateral mobility of plasmalemmal G protein-coupled cholecystokinin receptors. *J Fluorescence* **11:**237–246.

Roettger BF, Rentsch RU, Pinon D, Holicky E, Hadac EM, Larkin JM, and Miller LJ (1995) Dual pathways of internalization of the cholecystokinin receptor. *J Cell Biol* **128:**1029–1042.

Rosenzweig SA, Miller LJ, and Jamieson JD (1983) Identification and localization of cholecystokinin-binding sites on rat pancreatic plasma membranes and acinar cells: a biochemical and autoradiographic study. *J Cell Biol* **96:**1288–1297.

Rye HS (2001) Application of fluorescence resonance energy transfer to the GroEL-GroES chaperonin reaction. *Methods* **24:**278–288.

Stryer L and Haugland RP (1967) Energy transfer: a spectroscopic ruler. *Proc Natl Acad Sci USA* **58:**719–726.

Vallotton P, Tairi AP, Wohland T, Friedrich-Benet K, Pick H, Hovius R, and Vogel H (2001) Mapping the antagonist binding site of the serotonin type 3 receptor by fluorescence resonance energy transfer. *Biochemistry* **40:**12237–12242.

Address correspondence to: Dr. Laurence J. Miller, Director, Cancer Center, Department of Molecular Pharmacology and Experimental Therapeutics, Mayo Clinic Scottsdale, 13400 East Shea Boulevard, Scottsdale, AZ 85259. E-mail: miller@mayo.edu